Environmental Science and Pollution Research (2021) 28:16470–16479
https://doi.org/10.1007/s11356-020-11842-5

RESEARCH ARTICLE

Eco-friendly ionic liquid imprinted polymer based on a green synthesis strategy for highly selective adsorption tylosin in animal muscle samples

Lifang Wang[1] · Jingfan Chen[1] · Xian Li[1] · Letian Chen[1] · Kaige Zhang[1] · Xuefeng Wang[1] · Guifen Zhu[1]

Received: 8 September 2020 / Accepted: 25 November 2020 / Published online: 2 January 2021

Abstract

A novel eco-friendly molecularly imprinted polymer (MIP) was proposed as solid-phase extraction (SPE) adsorbent to selective adsorption tylosin (TYL) in animal muscle samples. The MIP was synthesized in aqueous by using 1,4-butanediyl-3,3-bis-1-vinyl imidazolium chloride and 2-acrylamide-2-methylpropanesulfonic acid as bifunctional monomer. The obtained MIP had excellent selectivity towards TYL in water, and the maximum binding capacity can reach 123.45 mg g^{-1}. Combined with high-performance liquid chromatography, the presented MIP can be used as SPE sorbent to recognize and detect TYL in the range of 0.008 to 0.6 mg L^{-1} ($R^2 = 0.9995$). The limit of detection and limit of quantification were 0.003 mg L^{-1} and 0.008 mg L^{-1}, and the intraday and interday precision were 1.05% and 3.36%, respectively. Under the optimal condition, the established MIP-SPE-HPLC method was successfully applied to separate and determine trace TYL in chicken, pork, and beef samples with satisfactory recoveries ranged from 94.0 to 106.3%, and the MIP-SPE cartridge can be cycled at least 20 times. This study implies a promising green MIP-SPE-HPLC method for highly selective adsorption and analysis trace TYL in complex matrices.

Keywords Eco-friendly · Imprinted polymer · Adsorption · Tylosin · Ionic liquids · Solid-phase extraction

Introduction

Tylosin (TYL) belongs to the sixteen-membered ring macrolide antibiotics. Owing to its low price, broad-spectrum, and high-efficiency antibacterial properties (Dong et al. 2018), TYL has been widely used as veterinary medicine for the treatment of animal disease and promoting of growth (Hume and Donske 2017). However, more than 50% of the used TYL antibiotics are discharged into environment in the form of prototypes or metabolites (Aust et al. 2008; Guo et al. 2014; Wegst-Uhrich et al. 2014). Although these antibiotic residues in environment are usually at concentration of μg L^{-1} or ng L^{-1} (Chen et al. 2019), the residues will enter the ecosystem or human body through various pathways such as material transfer and bioaccumulation, which will lead to the spread of antibiotic resistance and endanger human health (Wang and Wang 2015). Therefore, effective analysis and separation of macrolide antibiotic residues in environment have received increasing attention.

Up to now, the analytical methods for macrolide antibiotics include enzyme-linked immunosorbent assay (Xu et al. 2017), thin-layer chromatography (Ahmed et al. 2013), and high-performance liquid chromatography (Maher et al. 2008). Because the residual antibiotic in environment are often low in content, and it can be interfered by the coexisting substances, and so, effective separation and purification of samples are extensively required. Among the varieties of pretreatment technologies, solid-phase extraction (SPE) corresponding molecularly imprinted polymers (MIP) have attracted increasing attention.

MIP are synthetic functional material with specific recognition sites to target molecule. Due to the excellent selectivity, good stability, and easily preparation (Fan et al. 2020), MIP have received remarkable application in the fields of environmental monitoring, bioanalysis and food detection, sensors,

Responsible Editor: Tito Roberto Cadaval Jr

✉ Guifen Zhu
gfzhu617@163.com

[1] School of Environment, Henan Key Laboratory for Environmental Pollution Control, Key Laboratory for Yellow River and Huai River Water Environmental Pollution Control, Ministry of Education, Henan Normal University, Xinxiang 453007, Henan, People's Republic of China

solid-phase extraction, etc. (Ansari and Masoum 2019; Chrzanowska et al. 2015; Feng et al. 2019; Guo et al. 2018a; Motia et al. 2019). Zheng et al. (2011) developed a MIP for monitoring tilmicosin in feeds. It was found that the polymer sorbent can effectively extract and enrich tilmicosin in complicated feeds with satisfactory recovery. Song et al. (2016) synthesized a MIP using tylosin as the virtual template to extract macrolide drugs in animal muscle (swine, cattle, and chicken) samples, and the results showed that the MIP can highly recognize the residual antibiotics in theses samples. Although these MIP exhibit specific recognition performance towards targets, they were prepared in toxic organic solvents, such as chloroform and toluene, and the selective recognition of MIP in aqueous matrices can be significantly decreased, which will hinder the application of MIP in environmental fields (Cao et al. 2019; Fang et al. 2010). Thus, the development of MIP in green media is a good way to extend the application of imprinting materials in environmental systems.

Recently, some hydrophilic MIP have been prepared by using methacrylic acid or 2-acrylamido-2-methylpropanesulfonic acid as functional monomer (Piletsky et al. 2000; Shen and Ye 2011). However, these MIP with traditional monomer still have poor selectivity in water because water molecules with strong polarity can interfere with the interaction between imprinted molecule and functional monomer (Feng et al. 2018). It was reported that the synthesis of MIP is mainly relied upon the polymerization between functional monomer and template molecule. After removing imprinting molecule, MIP can generate recognition sites complementary to the imprinted molecule in chemically and sterically (Xu et al. 2019). Therefore, the appropriate monomer with multiple functional groups is the key for the synthesis of green MIP with superior selectivity in aqueous media.

Ionic liquids (ILs) are magic compounds composed only of cations and anions (Miao et al. 2017). Due to the advantages of negligible vapor pressure, high chemical/thermal stability, low melting point, and powerful dissolution ability, ILs have been extensively used in extraction, polymerization, and catalysts (Cumplido et al. 2020; Han et al. 2019; Zhu et al. 2019) Especially, those ILs with functional groups can form multiple interaction with target molecules to resist the interference of water molecules, and thus, preparation of hydrophilic MIP using ILs as functional monomer has recently attracted great interest. For example, Afzali et al. (2019) developed a novel MIP/Au/GO electrochemical sensor by using [VAIM]+Br^- as functional monomer for the determination of imiquimod in ethanol/water. Results indicated that MIP with particular sites improves the selectivity and can recognize imiquimod in real samples. A water compatible IL (1-allyl-3-vinylimidazole chloride)-based MIP was proposed by Zhu et al. (2019). The obtained MIP can selectively rebind quinolones in soil, water, and pork samples with recoveries in the range of 87.33–102.50%. Chen et al. (2019) introduced several amino acid chiral ILs as functional monomers to obtain MIP in water/methanol. It is found that the selectivity of L-Phe@MIP was obviously enhanced (102.7%) compared with non-imprinted polymer (NIP). This result indicated that ILs can be selected as novel functional monomers to synthesize green MIP with excellent selectivity in water. To the best of our knowledge, the eco-friendly MIP prepared using ILs as functional monomers to recognize TYL in animal muscle has not been reported.

Therefore, in this work, a novel eco-friendly MIP was presented in water by using 1,4-butanediyl-3,3-bis′-1-vinyl imidazolium chloride and 2-acrylamide-2-methylpropanesulfonic acid as bifunctional monomer for the specific adsorption of TYL in animal muscle samples. The resulting MIP was well characterized and the selectivity was investigated through equilibrium binding experiment. Under the optimal conditions, the as-prepared MIP was employed as solid-phase extraction sorbent combined with HPLC to effectively separate and detect TYL in chicken, pork, and beef samples.

Experimental

Materials and reagents

Tylosin was obtained from Chengdu Qiankun Animal Medicine Co., Ltd. (Chengdu, China). Poly(styrene-divinylbenzene) particle (40–60 μm) was supplied by Shanghai Boshi Biotech Co., Ltd. (Shanghai, China). 1-Vinylimidazole and 1,4-dichlorobutane were provided by Aladdin Industrial Inc. Ltd. (Shanghai, China). 2-Acrylamido-2-methylpropanesulfonic acid and N,N′-methylenebisacrylamide were provided by J&K Chem. Ltd. (Shanghai, China). Methanol of chromatographic grade was supplied by Tedia Co. (Fairfield, USA), and pure water from Wahaha Co. Ltd. (Henan, China) was used for HPLC analysis.

Instruments

The morphology of polymers was characterized by a field emission scanning electron microscope (JSM-5610LV, JEOL). Fourier transform infrared (FT-IR) spectra (4000–400 cm^{-1}) were analyzed using an infrared spectrophotometer (Perkin-Elmer 983, Norwalk). The microstructure parameters of the polymers were observed by a nitrogen adsorption-desorption analyzer (BELSORP-Max, Osaka). The sample analysis was performed on HPLC-PDA with a reversed-phase column (C18 column, 4.6 × 250 mm i.d., 5 μm particle size, Waters) in this work.

Synthesis of imprinted polymer

Three functionalized ionic liquids, such as 1,6-butanediyl-3,3′-bis-1-vinyl imidazolium bromine ([BIM-6C]Br), 1,4-

butanediyl-3,3-bis′-1-vinyl imidazolium chloride ([BIM-4C]Cl), and 1-vinyl-3-acetic acid imidazolium bromide ([COOHevim]Br), were synthesized according to the modified reported method (see Figure S1 in supplementary material).

In a typical procedure of preparing imprinted material, 0.15 g of poly(styrene-divinylbenzene) (PS-DVB, carrier), 0.4956 g of tylosin (TYL, template molecule), and 0.3152 g of ionic liquid and 0.1035 g 2-acrylamide-2-methylpropanesulfonic acid (AMPS) as co-functional monomer were added in water followed by polymerization for 4 h at 30 °C. Afterwards, 0.5781 g of N,N′-methylenebisacrylamide (MBA, crosslinker) and azobisisobutyronitrile (AIBN, initiator) were dissolved into the above solution and deoxygenated with nitrogen for 5 min. Subsequently, the polymerization was carried out in water bath at 60 °C for 24 h. The obtained product was then washed with a mixture of methanol-acetic acid (8:2, V:V) to remove the template molecule. After dried under a vacuum for 24 h at 60 °C, the MIP was obtained. Simultaneously, the non-imprinted polymer (NIP) was prepared in the same manner as MIP except no addition of the imprinted molecule.

Adsorption test

Equilibrium adsorption experiment was performed to investigate the binding property. The MIP and NIP (10 mg) were separately dipped into 10 mL TYL aqueous solution in the range of 1.58–396.46 mg L^{-1} followed by shaken for 3 h at 25 °C, 35 °C, 45 °C, and 55 °C, respectively; the supernatants were measured by HPLC at 290 nm. The mobile phase was a mixed solution of methanol-water-acid (57:43:0.001, v:v:v) with the flow rate of 1.0 mL min^{-1} at 30 °C, and the adsorption capacity Q_e of TYL on MIP and NIP was calculated based on equation $Q_e = 1000(C_i - C_e)V/m$ (Silva et al. 2016; Zhu et al. 2019). The adsorption kinetics of polymers was carried out according to the equilibrium adsorption experiment at the concentration of 25 mg L^{-1} at 25 °C, 35 °C, 45 °C, and 55 °C, respectively, and binding amount was calculated at different time intervals in 5–480 min by the equation $Qt = 1000(Ci - Ct)V/m$ (Alves et al. 2019).

Selective adsorption

The selectivity of imprinted material was performed according to equilibrium adsorption experiment. Herein, MIP and NIP (10 mg) were separately dispersed in a 10-mL mixed aqueous solution containing 0.05 mmol L^{-1} of tylosin (TYL), tilmicosin (TIL), kitasamycin (KITA), and metronidazole (MTZ). After shaking at 25 °C for 3 h, the concentration of different substrate was detected by HPLC.

Solid-phase extraction experiment

The MIP (120 mg) was packed into a 3-mL empty polypropylene tube to make a MIP-SPE cartridge. Before usage, the SPE cartridge was firstly conditioned by methanol, and 0.2 mg L^{-1} of TYL aqueous solution (10 mL) was loaded onto it. After that, the cartridge was washed with 2-mL acetonitrile-water-acetic acid (80/20/0.2, v:v:v) solution, and the eluates were then collected and measured by HPLC.

Sample pretreatment

Three samples including chicken, pork, and beef purchased from a local market were chosen to assess the separation performance of the MIP-SPE cartridge. The sample pretreatment process was as follows: each homogenized sample (5 g) was separately placed into a centrifuge tube and extracted by acetonitrile (3 mL), respectively. The mixture was successively vortexed (1 min), ultrasonicated (5 min), and then centrifugated (5 min) at 5000 rpm. Subsequently, the supernatant was transferred to another tube, and the above extraction steps were repeated once (Li et al. 2017). Afterwards, the above-obtained supernatant was mixed, evaporated till near dry, and dissolved in 10 mL water. Finally, the spiked samples were separately passed through the home-made MIP-SPE cartridge with the flow rate of 1.0 mL min^{-1}, and the content of TYL in elution was determined by HPLC.

Results and discussion

Optimization of polymerization conditions

To obtain the imprinted polymer with better performance, seven types of functional monomers, such as [BIM-6C]Br, [BIM-4C]Cl, [COOHevim]Br, AMPS, [BIM-6C]Br+AMPS, [BIM-4C]Cl+AMPS, and [COOHevim]Br+AMPS, were separately used to prepared polymers. The results in Table 1 displayed that the adsorption capacity (Q_e) and imprinting factor (α) of the MIP (MIP7-16) prepared with the co-functional monomer [BIM-4C]Cl+AMPS were obviously better than those synthesized using other monomer, and the higher Q_e and α were obtained at the molar ratio of 2:1 for [BIM-4C]Cl to AMPS (MIP7-16). It may be attributed to the introduce of the imidazole ring and sulfonic acid group in the co-functional monomer, which is beneficial to form ionic bond, hydrogen bond, and π-π interactions between MIP and TYL.

Additionally, the molar ratios of imprinted molecule to co-functional monomer (1:4, 1:6, 1:8, 1:10) and crosslinker (1:10, 1:15, 1:20, 1:25) were also investigated, respectively. The result listed in Table 1 indicated that the superior binding capacity (44.80 μmol g^{-1}) and imprinted factor (35.00) were

Table 1 Effect of preparation parameters on adsorption properties of MIP for TYL

MIP	Template (mmol)	Functional monomer (mmol)				Crosslinker (mmol)	Q_e (μmol g^{-1})	α^e
		[BIM-6C]Br[a]	[BIM-4C]Cl[b]	[COOHevim]Br[c]	AMPS[d]			
MIP1	0.25	1	0	0	0	5	23.41	4.46
MIP2	0.25	0	1	0	0	5	48.71	1.14
MIP3	0.25	0	0	1	0	5	17.10	6.28
MIP4	0.25	0	0	0	1	5	23.29	2.54
MIP5	0.25	0.5	0	0	0.5	5	13.14	27.95
MIP6	0.25	0	0	0.5	0.5	5	28.00	2.05
MIP7	0.25	0	0.5	0	0.25	5	31.69	12.28
MIP8	0.25	0	0.33	0	0.67	5	29.74	9.78
MIP9	0.25	0	0.67	0	0.33	5	36.15	15.38
MIP10	0.25	0	0.33	0	0.17	5	23.83	7.64
MIP11	0.25	0	1	0	0.5	5	44.80	35.00
MIP12	0.25	0	1.33	0	0.67	5	46.88	33.97
MIP13	0.25	0	1.67	0	0.83	5	47.11	10.07
MIP14	0.25	0	1	0	0.5	2.5	30.34	16.31
MIP15	0.25	0	1	0	0.5	3.75	41.53	30.99
MIP16	0.25	0	1	0	0.5	6.25	37.12	22.91

[a] [BIM-6C]Br is 1,6-butanediyl-3,3′-bis-1-vinyl imidazolium bromine

[b] [BIM-4C]Cl is 1,4-butanediyl-3,3-bis′-1-vinyl imidazolium chloride

[c] 1-vinyl-3-acetic acid imidazolium bromide

[d] 2-acrylamide-2-methylpropanesulfonic acid

[e] α is the imprinting factor, $\alpha = Q_{MIP}/Q_{NIP}$

obtained at a ratio of 1:6:20 (imprinted molecular to co-functional monomer to crosslinker) (MIP 11), which was the best ratio for the preparation of the imprinted polymer.

Characterization

FT-IR spectra of the PS-DVB, MIP, NIP, TYL, [BIM-4C]Cl, and AMPS are displayed in Figure S2. The peaks of MIP and NIP (curves b and c) at 2926 cm^{-1} corresponding to the stretch vibration of saturated C-H and -CH_2 in PS-DVB (curve a) (Liu and Liu 2001), indicating that the polymerization layer was successfully coated on the surface of carrier. Compared with the infrared data of each functional monomer, the absorbance in MIP and NIP at 1184 and 1038 cm^{-1} (curve b and c) were separately ascribed to the imidazole ring in [BIM-4C]Cl (Zhuo et al. 2016) and -SO_3H in AMPS (Anirudhan et al. 2017). And the peaks of imidazole ring and -SO_3H at 1179 cm^{-1} and 1075 cm^{-1} (curves e and f) shifted due to the polymerization reaction (Ma et al. 2018), which verified that [BIM-4C]Cl and AMPS were successfully incorporated into the polymerization layer. In addition, there was no characteristic adsorption peak of lactone carbonyl of TYL (1718 cm^{-1}, curve d) in MIP, revealing the completely elution of template molecule. These results illustrated that the imprinted materials based on co-functional monomers have been successfully obtained.

Figure 1 exhibits the surface images of MIP and NIP. It showed that MIP (Fig. 1a and b) and NIP (Fig. 1c and d) both have rough surface, and the polymer layer has good thermal stability (Figure S3). The difference verified that the carrier was successfully coated by polymeric layer. Furthermore, N_2 adsorption-desorption experiment demonstrated that the polymer layer has porous structure. Although the pore volume and size of MIP and NIP in Table S1 were close to each other, the adsorption capacity of MIP for TYL was much higher than that of NIP, which indicated that the porous on the surface of MIP can effectively rebind template molecules.

Adsorption properties

Figure 2a reveals that the binding capacity of MIP for TYL increased with the enhancing of initial substrate concentration, and the binding amount of TYL onto MIP also increased with the increase of temperatures. More importantly, the presented MIP was more eco-friendly and had higher adsorption capacity (123.45 mg g^{-1}) towards TYL than those of reported

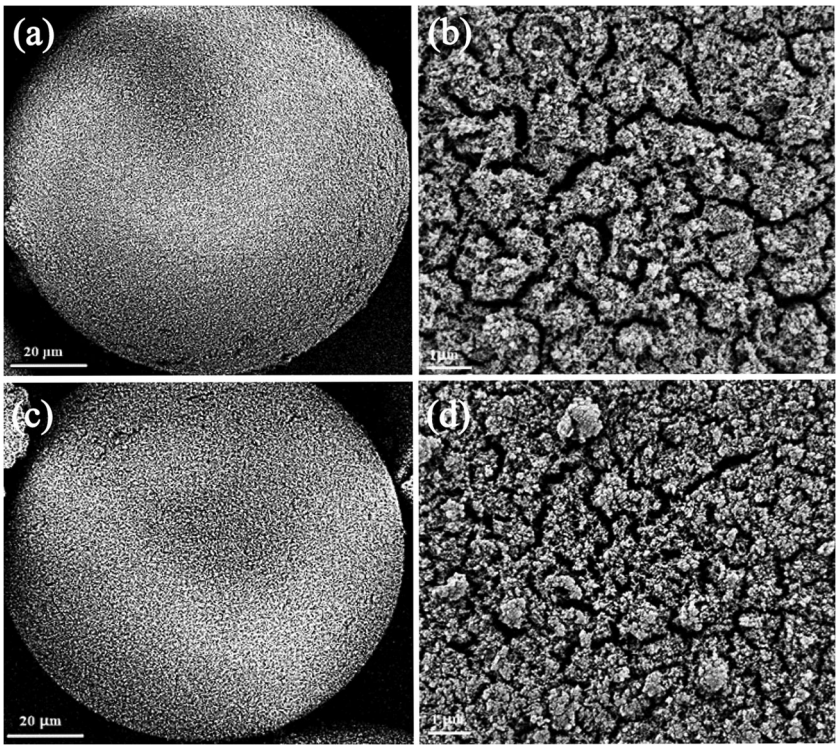

Fig. 1 SEM images of MIP (**a** and **b**) and NIP (**c** and **d**)

adsorbent in Table 2. On the contrary, the adsorption process of NIP for TYL varied little with the increase of concentration and temperature, and the Q_e values were significantly lower than that of MIP.

The adsorption kinetics curves (Fig. 2b) showed that the binding amount of TYL onto MIP enhanced with the extension of adsorption time, and Q values were close to equilibrium at 240 min. This phenomenon might be due to the existence of a great quantity of adsorption sites on MIP at initial time, and the adsorption rate of MIP for TYL decreased gradually with the occupation of imprinting sites. Additionally, the adsorption capacities of MIP for TYL increased with the increase of experimental temperatures, indicating that the increase of temperature was beneficial to the adsorption. In contrast, the adsorption of TYL on NIP was poor and little affected by contact time and temperature. This result illustrated that the prepared MIP has better imprinting performance, and can be a promising adsorbent for removing TYL from real samples.

Selectivity

The selectivity of polymer towards single substrate was performed according to equilibrium adsorption experiment (see Figure S5 in supplementary material). It was found that the prepared MIP had excellent rebinding amount towards tylosin (TYL) and tilmicosin (TIL) and kitasamycin (KITA), while the adsorption for metronidazole (MTZ) and amoxicillin (AMX) was very poor. This result suggested that the binding sites on MIP were specific to TYL and its analogues. Furthermore, the recognition of MIP and NIP in complex water matrix was also performed, and the partition coefficient (K_d), selectivity coefficient (K), and relative selectivity coefficient (K′) (Xie et al. 2015) were employed to evaluate the recognition ability.

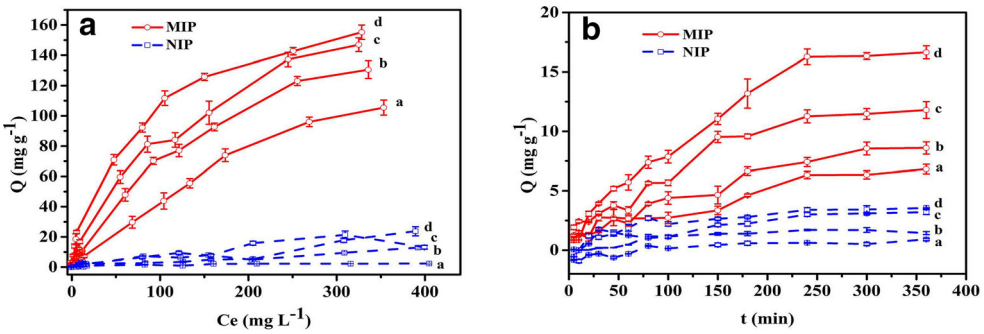

Fig. 2 Adsorption isotherm curves (**a**) and kinetic adsorption curves (**b**) of MIP and NIP towards TYL (a, 25 °C; b, 35 °C; c, 45 °C; d, 55 °C) ([TYL] = 0.0008–0.2 mmol L^{-1}, $m_{MIP/NIP}$ = 10 mg)

Table 2 Comparison of adsorption properties of different adsorbents for TYL

Absorbent	Preparation solvent	Sample	Linearity (mg L^{-1})	Q_{max} (mg g^{-1})	Cycles	Reference
BCF	HCl, water	TYL solution	0.1–100	5.38	-	Guo et al. 2016
MS-ZnS:Mn	Water	TYL solution	-	3.45	-	Guo et al. 2018c
CCM-AC	Liquid paraffin	TYL solution	-	59.26	5	Luo et al. 2019
MPs	HCl, water	TYL solution	-	0.64–1.54	-	Guo et al. 2018b
MIP	Water	Chicken, pork, and beef	0.008–0.6	123.45	20	This work

$$K_d = Q_e/C_e \quad (1)$$

$$K = K_{d1}/K_{d2} \quad (2)$$

$$K' = K_{MIP}/K_{NIP} \quad (3)$$

where K_d represent the adsorption capacity of the polymer. K_{d1} and K_{d2} are the partition coefficients of TYL and the other coexisting substance, respectively. K′ indicates the selectivity difference between MIP and NIP.

It is found from Table S2 that MIP can effectively recognize TYL, TIL, and KITA in the mixed solution, and their K_d values (289.40, 209.30, and 448.81 mL g^{-1}) were significantly higher than that of MTZ (32.14 mL g^{-1}). And the K values of MIP for TIL and KITA (1.38 and 0.64) were close to 1, indicating that the MIP had similar recognition performance for these macrolide antibiotics. The probably reason was that TYL, TIL, and KITA had the same macrolide structure, which can match the specific affinity sites formed by TYL in MIP, and so they all can be effectively identified. However, the structure of coexisting MTZ was very different from that of the template molecule, and there was only non-specific adsorption so that the K_d value was very lower. Furthermore, K′ value (7.50) illustrated that the selectivity of MIP was almost 8 times that of the NIP, which indicated that the employment of IL functional monomer remarkably improved the selectivity of MIP in water matrix, and which was favorable for the application of MIP in environmental system.

Adsorption mechanism

To discuss the adsorption mechanism of MIP, the adsorption of TYL onto MIP at different pH was investigated and shown in Fig. 3a. It can be observed that the binding capacity remained stable (~ 13 mg g^{-1}) with the pH increase within 3.0–7.0, while the adsorption capacity enhanced remarkably to ~ 30 mg g^{-1} as the pH increase to 10.0. This effect of pH on the adsorption of MIP can be explained by the zero point charge (pH_{zpc}). Figure 3a shows that the pH_{zpc} value of MIP was 7.6, which means that the net surface charge of the MIP is positive when pH value is below 7.6, while above which is negative (Zhu et al. 2019). It is reported that TYL^+ with positive charge was the main existing form when pH value is lower than 7.1, and the neutral molecular TYL° constitute the majority when pH value is greater than 7.1 (Luo et al. 2019). Hence, when the pH value of solution is less than 7.0, the charge repulsion between MIP and TYL leads to the lower adsorption capacity, while when pH > 7.0, MIP with negative charge can attract neutral molecular TYL°, which is contribute to the rebinding of TYL onto MIP.

Additionally, the FT-IR spectra of MIP-YLT in Fig. 3b displayed that the stretching vibration of C=N (1529 cm^{-1}) and C-H (3066 cm^{-1}) on ionic liquid of MIP shifted to 1532 cm^{-1} and 3059 cm^{-1} after the adsorption for TYL, which indicated that hydrogen bond had formed between the ionic liquid of MIP and TYL (Zhu et al. 2019). And the molecule of TYL contains abundant carbonyl and hydroxyl groups which can be used as hydrogen acceptors or donors (Guo et al. 2013). This result suggested that hydrogen bond plays an important role in recognition of MIP for TYL. Moreover, TYL and IL of MIP both have ring structures, and π-π interaction might be formed between lactone and aromatic rings of TYL and the imidazole rings of TYL. Furthermore, XPS spectra of imprinted material before (MIP) and after adsorption of TYL (MIP-TYL) in C 1s was characterized. In Fig. 3c, the strong peak at 284.7 eV is ascribe to C-C, and the peaks at 285.9 eV, 286.9 eV, and 287.8 eV are separately caused by C-N, C=N, and C=O. Compared with the spectra in Fig. 3c, there is one additional C-O peak at 288.1 eV in Fig. 3d, indicating that the specific binding sites in MIP have effectively adsorbed TYL which contains C-O group. Hence, the synergistic effect of electrostatic, hydrogen bond, and π-π interaction enable MIP to effectively recognize TYL in aqueous media.

Optimization of MIP-SPE cartridge

The flow rate can significantly affect the separation and enrichment efficiency of the solid-phase extraction cartridge for

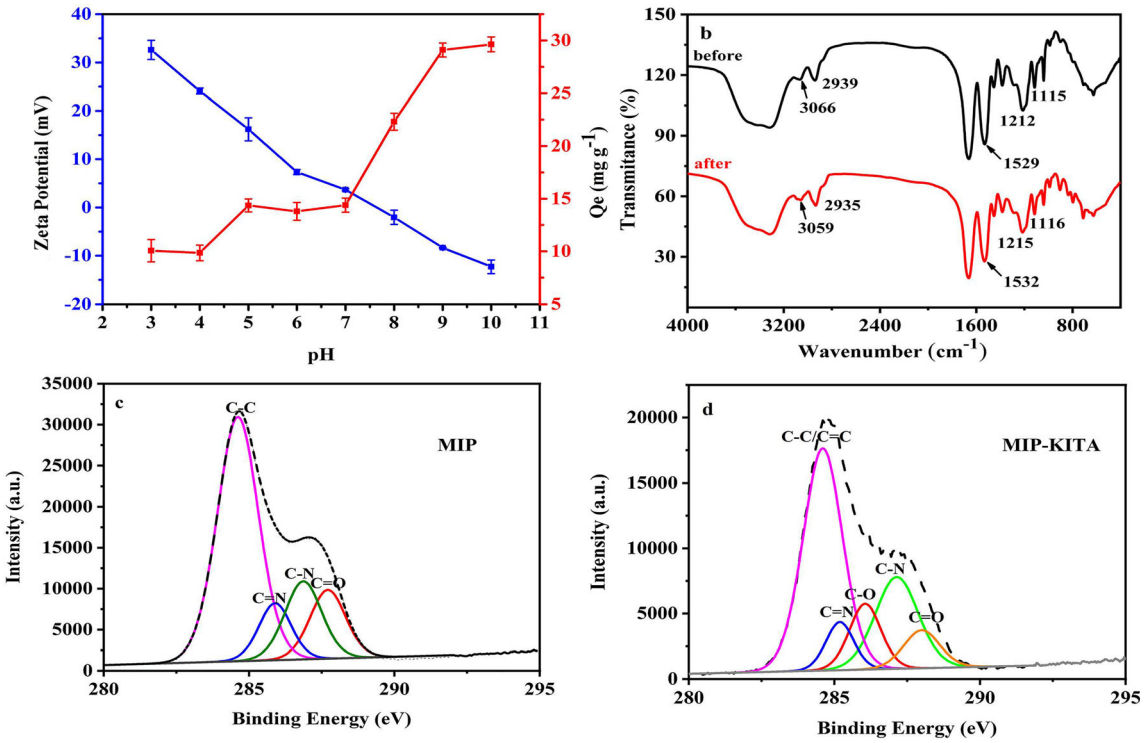

Fig. 3 Effect of pH values on zeta potential of MIP (**a**), FT-IR of MIP before and after adsorption of TYL (**b**), and XPS analysis of MIP before (**c**) and after adsorption of TYL (**d**) ([TYL] = 50 mg L^{-1}, m_{MIP} = 10 mg)

target. To explore the optimal loading rate, 10-mL TYL aqueous solution (0.2 mg L^{-1}) was loaded into the MIP-SPE cartridge in the flow rate range from 0.5 to 1.8 mL min^{-1} followed by eluting, and the content of TYL in eluents was determined by HPLC. It is found in Fig. 4a that nearly 100% of TYL was bounded onto the MIP-SPE cartridge when the loading flow rate was less than 1.2 mL min^{-1}, while the retention of TYL on the MIP-SPE cartridge decreased notably with increase of flow rate. Hence, 1.0 mL min^{-1} was selected as the optimized loading rate.

To discuss the appropriate elution solvent in this experiment, 5-mL TYL aqueous solution (0.2 mg L^{-1}) was passed through the cartridge, and then 5 mL of different solutions (methanol, methanol-water (9:1, V/V), methanol-water (8:2, V/V), methanol-water-acetic acid (80:20:0.2, V/V/V), acetonitrile, acetonitrile-water (9:1, V/V), acetonitrile-water (8:2, V/V), acetonitrile-water (7:3, V/V), acetonitrile-water-acetic acid (70:30:0.2, V/V/V), acetonitrile-water-acetic acid (80:20:0.2, V/V/V), and acetonitrile-water-acetic acid (90:10:0.2, V/V/V)) were used as eluent to dissolve TYL, respectively. From Fig. 4b, it was found that almost 100% TYL bounded on the MIP-SPE cartridge can be desorbed by acetonitrile-water-acetic acid (80:20:0.2, V/V/V), acetonitrile-water-acetic acid (90:10:0.2, V/V/V), and acetonitrile-water-

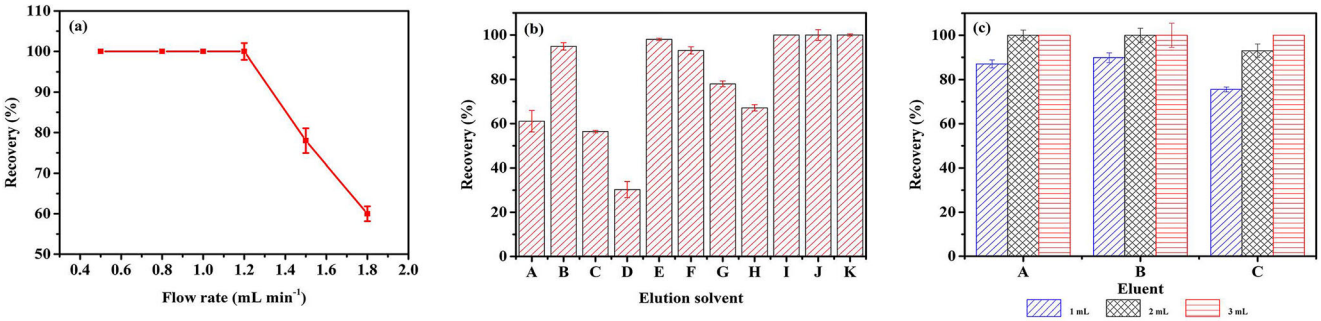

Fig. 4 Recovery of TYL on the MIP-SPE cartridge with different loading rate (**a**). Recoveries of TYL on the MIP-SPE cartridge when using different elution solvent: A, methanol; B, methanol:water (90:10); C, methanol:water (80:20); D, methanol:water:acid (80:20:0.2); E, acetonitrile; F, acetonitrile:water (90:10); G, acetonitrile:water (80:20); H, acetonitrile:water (70:30); I, acetonitrile:water:acid (90:10:0.2); J, acetonitrile:water:acid (80:20:0.2); K, acetonitrile:water:acid (70:30:0.2) (**b**). Recoveries of TYL on the MIP-SPE cartridge when using different volume of elution solvent: A, acetonitrile:water:acid (90:10:0.2); B, acetonitrile:water:acid (80:20:0.2); C, acetonitrile:water:acid (70:30:0.2) (**c**)

acetic acid (70:30:0.2). Therefore, the three mixture of acetonitrile-water-acetic acid can be used as the eluent.

In order to optimize the type and volume of eluent, different volumes (1 mL, 2 mL, 3 mL) of the above three eluents were applied to elute the TYL (10 mL, 0.2 mg L^{-1}), respectively. The analysis results in Fig. 4c indicated that 2 mL of mixture of acetonitrile-water-acetic acid (80:20:0.2, V/V/V) and acetonitrile-water-acetic acid (90:10:0.2, V/V/V) can completely desorb the TYL bound onto the SPE cartridge. Considering the pollution of organic reagents and higher enrichment ratio, 2 mL of acetonitrile-water-acetic acid (80:20:0.2, V/V/V) was employed as the eluent in this work.

Method validation

The validation of the above MIP-SPE-HPLC method was assessed by a series of parameters including linearity, limit of detection (LOD), limit of quantification (LOQ), and precision. As can be seen from Table S3, a good linearity for TYL was obtained ($R^2 = 0.9995$) in the range of 0.008 to 0.6 mg L^{-1}, and the LOD and LOQ were found to be 0.003 mg L^{-1} and 0.008 mg L^{-1}, respectively. The precision of the proposed method was evaluated by extracting the spiked sample solution (0.06 mg L^{-1}) on the same day and three consecutive days, and the intraday and interday precision were 1.05% and 3.36%, respectively. The above results indicated that the established analytical method has good reliability for recognition of TYL.

Application

The applicability of as-prepared MIP-SPE-HPLC for selective absorbing and analysis TYL in chicken, pork, and beef samples was checked. Under the optimized conditions, each 10-mL spiked sample (0.02 mg L^{-1}) was passed through the MIP-SPE cartridge, respectively, followed by eluted, and the chromatogram of eluent is shown in Fig. 5. It can be seen that no TYL was found in the original sample solutions (Fig. 5a, b, and c), while peaks of TYL in eluates of chicken (Fig. 5a'), pork (Fig. 5b'), and beef samples (Fig. 5c') can be clearly observed after extraction step. This result demonstrated that the separation and preconcentration process by the self-made MIP-SPE cartridge was contributed to the analysis of TYL in real samples.

The application of the MIP-SPE-HPLC method was further determined using a recovery experiment, and animal muscle samples that spiked three different concentration level of TYL (10 μg L^{-1}, 20 μg L^{-1}, 60 μg L^{-1}) were tested, respectively. The eluents were detected by HPLC and the results are listed in Table 3. The recovery of TYL was found in the range of 94.0–106.3%, and the relative standard deviation (RSD) was less than 6.4%.

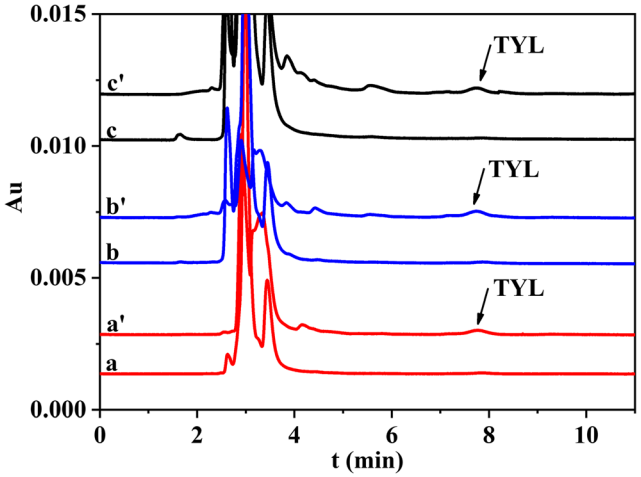

Fig. 5 Chromatograms of muscle samples spiked 20 μg L^{-1} TYL before and after MIP-SPE extraction. a, b, and c are the original solution of chicken, pork, and beef samples without extraction, and a′, b′, and c′ represent elution of chicken, pork, and beef samples after extraction, respectively (HPLC-UV conditions: HPLC-UV experiments were performed using a Wondasil C_{18} column (4.6 × 250 mm, 5 μm). The column temperature was maintained at 30 °C, the mobile phase was 57% methanol and 43% water (0.1% acetic acid), the injection volume and the flow rate were 20 μL and 1 mL min^{-1}, respectively, and the detection wavelength is 290 nm)

Regeneration of MIP-SPE cartridge

The regeneration of adsorbents is one of the most important criteria for the purpose of cost and efficiency (Dotto et al. 2016). In order to investigate the regeneration of the MIP-SPE cartridge, the adsorption-desorption procedure was repeated. Briefly, 10 mL (0.20 mg L^{-1}) of TYL aqueous solution was passed through the MIP-SPE cartridge under the optimized condition followed by washing with the mixed solution of acetonitrile-water-acetic acid (80:20:0.2, V/V/V).

Table 3 Recoveries of TYL in real environmental samples ($n = 3$)

Samples	Added (μg L^{-1})	Found (μg L^{-1}) ± SD	Recovery (%)	RSD (%)
Chicken	-	ND [a]	-	-
	10.0	9.9 ± 0.54	99.0	5.5
	20.0	19.7 ± 0.74	98.5	3.8
	60.0	63.8 ± 2.73	106.3	4.0
Pork	-	ND	-	-
	10.0	9.9 ± 0.63	99.0	6.4
	20.0	19.2 ± 1.17	96.0	6.1
	60.0	57.1 ± 1.77	95.2	3.1
Beef	-	ND	-	-
	10.0	9.4 ± 0.10	94.0	1.1
	20.0	19.3 ± 1.06	96.5	5.5
	60.0	56.9 ± 1.53	94.8	2.7

[a] ND is not detected

The concentration of TYL in eluent was measured using HPLC at 290 nm. The recovery of TYL by MIP-SPE was calculated based on the equation $R\% = C_a/C_b*100\%$; the C_a and C_b represent concentration of TYL after and before enrichment by MIP-SPE, and the result is shown in Figure S6 (Vieira et al. 2014). It can be clearly seen that approximately 90% of TYL can be obtained by this MIP-SPE cartridge after 20 cycles, confirming that the presented MIP with good stability and regeneration in this work can achieve high-efficiency separation and enrichment of TYL in complex samples.

Conclusion

In summary, we developed a newly eco-friendly MIP as SPE sorbent for highly selective extraction tylosin (TYL) in water. After optimizing the parameters affecting SPE procedure, a MIP-SPE-HPLC method was proposed to extract and detect TYL from in chicken, pork, and beef samples with high recoveries of 94.0–106.3% and the RSD was less than 6.4%, and the MIP-SPE cartridge can also be recycled with simple treatment. By embedding ionic liquid into the imprinted material, the MIP with multiple recognition sites acquired high binding capacity and excellent aqueous applicability, which possessed impressive merits of no toxicity, no organic solvent, and environmentally friendly reaction conditions. The established green and easily MIP-SPE-HPLC strategy can be expected for highly selective adsorption and analysis water-soluble contaminate in various food matrixes.

Supplementary Information The online version contains supplementary material available at https://doi.org/10.1007/s11356-020-11842-5.

Authors' contributions All authors contributed to the study conception and design. Material preparation, data collection, data analysis, and first draft of the manuscript were performed by Lifang Wang and Jingfan Chen. Investigation and software were performed by Xian Li and Letian Chen. The financial support for the project, critical review, commentary, or revision were performance by Kaige Zhang, and Guifen Zhu. The ideas and formulation of overarching research goals and aims were performance by Xuefeng Wang and Guifen Zhu. All authors commented on previous versions of the manuscript. All authors read and approved the final manuscript.

Funding This work was financially supported by the National Natural Science Foundation of China (nos. 21876045, 21507023, and 21605040), Science and Technology Department of Henan Province (no. 182102310656), and Program for Innovative Research Team in Science and Technology in University of Henan Province (no. 20IRTSTHN011).

Compliance with ethical standards

Competing interests The authors declare that they have no competing interests.

Ethics approval and consent to participate Not applicable

Consent for publication Not applicable

References

Afzali M, Mostafavi A, Shamspur T (2019) Developing a novel sensor based on ionic liquid molecularly imprinted polymer/gold nanoparticles/graphene oxide for the selective determination of an anticancer drug imiquimod. Biosens Bioelectron 143:111620

Ahmed MBM, Sree YHA, Abdel-Fattah SM, Hassan NS, Saad MME (2013) Determination of tylosin, spiramycin, and erythromycin residues in egyptian buffaloes' meat by thin-layer chromatography-bioautography. JPC J Planar Chromatogr-Mod TLC 26(5):409–416

Alves DCS, Gonçalves JO, Coseglio BB, Burgo TAL, Dotto GL, Pinto LAA, Cadaval TRS Jr (2019) Adsorption of phenol onto chitosan hydrogel scaffold modified with carbon nanotubes. J Environ Chem Eng 7(6):103460

Anirudhan TS, Christa J, Deepa JR (2017) Extraction of melamine from milk using a magnetic molecularly imprinted polymer. Food Chem 227:85–92

Ansari S, Masoum S (2019) Molecularly imprinted polymers for capturing and sensing proteins: current progress and future implications. TrAC Trends Anal Chem 114:29–47

Aust MO, Godlinski F, Travis GR, Hao XY, McAllister TA, Leinweber P, Thiele-Bruhn S (2008) Distribution of sulfamethazine, chlortetracycline and tylosin in manure and soil of Canadian feedlots after subtherapeutic use in cattle. Environ Pollut 156(3):1243–1251

Cao JK, Wang MW, Han DD, Qiao FX, Yan HY (2019) Attapulgite/hydrophilic molecularly imprinted monolithic resin composite for the selective recognition and sensitive determination of plant growth regulators in cucumbers. Food Chem 297:124974

Chen SY, Huang XX, Yao S, Huang WC, Xin Y, Zhu MH, Song H (2019) Highly selective recognition of L-phenylalanine with molecularly imprinted polymers based on imidazolyl amino acid chiral ionic liquid. Chirality 31(10):824–834

Chrzanowska AM, Poliwoda A, Wieczorek PP (2015) Surface molecularly imprinted silica for selective solid-phase extraction of biochanin A, daidzein and genistein from urine samples. J Chromatogr A 1392:1–9

Cumplido MP, Cháfe A, de la Torre J, Poy H (2020) Separation of the azeotropic mixture 2-propanol + water employing different imidazolium ionic liquids as solvents. J Chem Thermodyn 140:105889

Dong H, Yin YY, Guo XT (2018) Synthesis and characterization of Ag/Bi2WO6/GO composite for the fast degradation of tylosin under visible light. Environ Sci Pollut R 25(12):11754–11766

Dotto GL, Rodrigues FK, Tanabe EH, Fröhlich R, Bertuol DA, Martins TR, Foletto EL (2016) Development of chitosan/bentonite hybrid composite to remove hazardous anionic and cationic dyes from colored effluents. J Environ Chem Eng 4(3):3230–3239

Fan YM, Zeng GL, Ma XG (2020) Multi-templates surface molecularly imprinted polymer for rapid separation and analysis of quinolones in water. Environ Sci Pollut R 27(7):7177–7187

Fang GZ, Chen J, Wang JP, He JX, Wang S (2010) N-methylimidazolium ionic liquid-functionalized silica as a sorbent for selective solid-phase extraction of 12 sulfonylurea herbicides in environmental water and soil samples. J Chromatogr A 1217(10):1567–1574

Feng XT, Ashley J, Zhou TC, Sun Y (2018) Fluorometric determination of doxycycline based on the use of carbon quantum dots incorporated into a molecularly imprinted polymer. Microchim Acta 185(11):500

Feng ZM, Wang Y, Yang L, Sun T (2019) Coupling mesoporous imprinted polymer based DGT passive samplers and HPLC: a new tool for in-situ selective measurement of low concentration tetrabromobisphenol A in freshwaters. Sci. Total Environ 685: 442–450

Guo XT, Yang C, Dang Z, Zhang Q, Li YJ, Meng QY (2013) Sorption thermodynamics and kinetics properties of tylosin and sulfamethazine on goethite. Chem Eng J 223:59–67

Guo XT, Yang C, Wu YN, Dang Z (2014) The influences of pH and ionic strength on the sorption of tylosin on goethite. Environ Sci Pollut R 21(4):2572–2580

Guo XT, Dong H, Yang C, Zhang Q, Liao CJ, Zha FG, Gao LM (2016) Application of goethite modified biochar for tylosin removal from aqueous solution. Colloid Surface A 502:81–88

Guo HQ, Liu Y, Ma WT, Yan LS, Li KX, Lin S (2018a) Surface molecular imprinting on carbon microspheres for fast and selective adsorption of perfluorooctane sulfonate. J Hazard Mater 348:29–38

Guo XT, Pang JW, Chen SY, Jia HZ (2018b) Sorption properties of tylosin on four different microplastics. Chemosphere 209:240–245

Guo XT, Yin YY, Yang C, Dang Z (2018c) Maize straw decorated with sulfide for tylosin removal from the water. Ecotox Environ Safe 152: 16–23

Han BY, Jiang JH, Zhang WD, Yin F, Liu SQ, Zhao XL, Liu J, Wang CM, Yang H (2019) Hydrolysis of rapeseed oil to fatty acids using pyrrolidonium ionic liquids as catalysts. Energ Source Part A 41(20):2448–2459

Hume ME, Donske CJ (2017) Effect of vancomycin, tylosin, and chlortetracycline on vancomycin-resistant Enterococcus faecium colonization of broiler chickens during grow-out. Foodborne Pathog Dis 14(4):231–237

Li YQ, D HY, W JT, Q C, D KQ, H YY, H YM (2017) Synchronous fluorimetric determination of residue Ceftiofur in pig muscle and kindey by alkaline degradation and sensibilization. Food Res Dev 38(10):113–117

Liu FW, Liu YK (2001) IR spectroscopic study on chloromethylated styrene-divinylbenzene copolymer. Henan science 19:56–58

Luo XG, Liu LM, Wang LR, Liu XT, Cai YX (2019) Facile synthesis and low concentration tylosin adsorption performance of chitosan/cellulose nanocomposite microspheres. Carbohydr Polym 206: 633–640

Ma JK, Huang XC, Wei SL (2018) Preparation and application of chlorpyrifos molecularly imprinted solid-phase microextraction probes for the residual determination of organophosphorous pesticides in fresh and dry foods. J Sep Sci 41(15):3152–3162

Maher HM, Youssef RM, Khalil RH, El-Bahr SM (2008) Simultaneous multiresidue determination of metronidazole and spiramycin in fish muscle using high performance liquid chromatography with UV detection. J Chromatogr B 876(2):175–181

Miao QC, Bi EP, Li BH (2017) Roles of polar groups and aromatic structures of biochar in 1-methyl-3-octylimidazolium chloride ionic liquid adsorption: pH effect and thermodynamics study. Environ Sci Pollut R 24(28):22265–22274

Motia S, Tudor IA, Ribeiro PA, Raposo M, Bouchikhi B, El Bari N (2019) Electrochemical sensor based on molecularly imprinted polymer for sensitive triclosan detection in wastewater and mineral water. Sci Total Environ 664:647–658

Piletsky SA, Matuschewski H, Schedler U, Wilpert A, Piletska EV, Thiele TA, Ulbricht M (2000) Surface functionalization of porous polypropylene membranes with molecularly imprinted polymers by photograft copolymerization in water. Macromolecules 33:3092–3098

Shen XT, Ye L (2011) Molecular imprinting in Pickering emulsions: a new insight into molecular recognition in water. Chem Commun 47(37):10359–10361

Silva JM, Farias BS, Grundmann DDR, Cadaval TRS Jr, Moura JM, Dotto GL, Pinto LAA (2016) Development of chitosan/Spirulina bio-blend films and its biosorption potential for dyes. J Appl Polym Sci 134(11):44580

Song XQ, Zhou T, Liu QY, Zhang MY, Meng CY, Li JF, He LM (2016) Molecularly imprinted solid-phase extraction for the determination of ten macrolide drugs residues in animal muscles by liquid chromatography-tandem mass spectrometry. Food Chem 208:169–176

Vieira MLG, Esquerdo VM, Nobre LR, Dotto GL, Pinto LAA (2014) Glass beads coated with chitosan for the food azo dyes adsorption in a fixed bed column. J Ind Eng Chem 20(5):3387–3393

Wang SL, Wang H (2015) Adsorption behavior of antibiotic in soil environment: a critical review. Front Environ Sci Eng China 9(4):565–574

Wegst-Uhrich SR, Navarro DAG, Zimmerman L, Aga DS (2014) Assessing antibiotic sorption in soil: a literature review and new case studies on sulfonamides and macrolides. Chem Cent J 8:5

Xie XY, Chen L, Pan XY, Wang SC (2015) Synthesis of magnetic molecularly imprinted polymers by reversible addition fragmentation chain transfer strategy and its application in the Sudan dyes residue analysis. J Chromatogr A 1405:32–39

Xu Y, Zhao Q, Jiang LY, Li ZQ, Chen YH, Ding L (2017) Selective determination of sulfonamides from environmental water based on magnetic surface molecularly imprinting technology. Environ Sci Pollut R 24(10):9174–9186

Xu JQ, Qiao XJ, Wang Y, Sheng QL, Yue TL, Zheng JB, Zhou M (2019) Electrostatic assembly of gold nanoparticles on black phosphorus nanosheets for electrochemical aptasensing of patulin. Microchim Acta 186(4):238

Zheng YQ, Liu YH, Guo HB, He LM, Zeng ZL (2011) Molecularly imprinted solid-phase extraction for determination of tilmicosin in feed using high performance liquid chromatography. Ana Chim Acta 690(2):269–274

Zhu GF, Cheng GH, Lu T, Cao ZG, Wang LF, Li QJ, Fan J (2019) An ionic liquid functionalized polymer for simultaneous removal of four phenolic pollutants in real environmental samples. J Hazard Mater 373:347–358

Zhuo KL, Ma XL, Chen YJ, Wang CY, Li AQ, Yan CL (2016) Molecularly imprinted polymer based potentiometric sensor for the determination of 1-hexyl-3-methylimidazolium cation in aqueous solution. Ionics 22(10):1947–1955